Proceedings, 11th FIG Symposium on Deformation Measurements, Santorini, Greece, 2003.

INTEGRATION OF LEVELING AND INSAR DATA FOR LAND SUBSIDENCE MONITORING

Dennis Odijk, Frank Kenselaar and Ramon Hanssen

Delft University of Technology, Department of Mathematical Geodesy and Positioning, Thijsseweg 11, 2629 JA Delft, The Netherlands

Abstract

Leveling surveys have traditionally been used for the geodetic monitoring of land subsidence. Although optical leveling allows for the detection of very small deformations, it is rather expensive and time-consuming. Because of the high temporal and spatial resolution versus relatively low costs, the interferometric use of Synthetic Aperture Radar (InSAR) is in principal a promising supplement for precise deformation monitoring. In this paper an integrated approach is described for the adjustment and testing of height differences from both leveling and InSAR data. This approach is restricted to subsidence due to gas or oil extraction, for which a smooth spatio-temporal subsidence bowl may be assumed and residual subsidence can be stochastically modeled. Test computations show that the velocity, shape and location of an isolated subsidence bowl due to oil extraction can be in good agreement when estimated from either leveling observations only or from combined leveling/InSAR observations. In such an integrated approach the number of leveling observations can be significantly reduced. Nevertheless, leveling data remain necessary, since the availability and quality of InSAR data cannot always be guaranteed yet.

1. Introduction

In many respects classic optical leveling and satellite interferometric SAR (InSAR) can be seen as complementary measurement techniques for monitoring land subsidence. Leveling provides height differences between well-defined benchmarks at specific epochs. The temporal resolution depends on the expected subsidence rate but is often quite low, e.g. yearly campaigns for monitoring land subsidence due to extraction of natural resources. However, for long-term subsidence processes leveling measurements or derived heights are often the only source of geodetic data. InSAR provides temporal height differences for coherent resolution. Depending on the conditions, the available data can have both a high spatial and temporal resolution. While leveling benchmarks, if well founded, represent subsoil deformations, the InSAR-derived height changes can originate from surface, subsoil or even building deformations, depending on the dominant source of the radar reflection. The different characteristics of leveling and InSAR data can be combined in an integrated subsidence analysis, possibly resulting in more efficient monitoring strategies.

Since a physical connection between leveling benchmarks and InSAR scatterers is usually impossible, the data integration is supported by adopting a *spatio-temporal* trend model for land subsidence due to gas or oil extraction. Discrepancies from this first-order approximation can be computed and visualized as remaining signal. Special attention needs to be paid to the stochastic model that not only accounts for measurement noise, but should also cover non-systematic point instability, model inaccuracies, and atmospheric noise.
In cooperation with the Dutch Oil Company NAM we developed *SuMo* (Subsidence Modeling), prototype software for the integrated processing of leveling and InSAR data to temporal height differences. The parameters of the kinematic subsidence model are computed by a rigorous least-squares estimation and the data from both sources are statistically tested for significant

outliers. The concepts of the integrated model will be discussed in this article, as well as first results. In Sect. 2 the observation equations for height differences from leveling and InSAR data are introduced. Section 3 specifies the spatio-temporal subsidence model, while Sect. 4 treats the estimation and testing procedure of the subsidence, as implemented in the *SuMo* software (Odijk and Kenselaar, 2002). In Sect. 5 test results are given for an isolated oilfield followed by concluding remarks in Sect. 6.

2. Observation equations for height differences from leveling and InSAR

The observation equation for a *leveled* height difference $\underline{h}_{ij,t}$ between benchmarks i and j at time t reads:

$$\underline{h}_{ij,t} = -\underline{H}_{i,t} + \underline{H}_{j,t} + \underline{\varepsilon}_{ij,t}, \tag{1}$$

where $\underline{H}_{i,t}$ denotes the height of benchmark i at epoch t, $\underline{H}_{j,t}$ the height of benchmark j at epoch t, and $\underline{\varepsilon}_{ij,t}$ the random measurement noise. The underscore emphasizes the stochastic nature of the quantities. It is assumed that all leveling benchmarks within a network at a certain epoch are stable with respect to each other.

The *InSAR-derived* height differences in this paper are assumed to reflect vertical deformations collected in a grid for the time interval between two InSAR acquisitions. It is assumed that the phase ambiguities have been correctly resolved. The observation equation for a height difference $\underline{dH}_{k,t_l t_m}$ reads as follows, for point k between epochs t_l and t_m:

$$\underline{dH}_{k,t_l t_m} = -\underline{H}_{k,t_l} + \underline{H}_{k,t_m} - dH_{t_l t_m} + \underline{\varepsilon}_{k,t_l t_m}. \tag{2}$$

Besides the heights of the points at the two epochs and a random measurement error in this equation a so-called *shift* parameter $dH_{t_l t_m}$ appears. This shift, which is equal for all data of a deformation map, models a possible height difference in reference points of the two images from which the deformation map is generated.

The heights of each point in Eqs. (1) and (2) can be written as a function of the *vertical deformation*, for point i at time t:

$$\underline{H}_{i,t} = H_{i,t_0} + \underline{g}_{i,t-t_0}. \tag{3}$$

In this expression H_{i,t_0} denotes the initial height of the point before the beginning of the subsidence at time t_0, whereas the term $\underline{g}_{i,t-t_0}$ accounts for the vertical deformation since the beginning of subsidence. This subsidence is decomposed into a *trend* $z_{i,t-t_0}$ and a *signal* $\underline{\xi}_{i,t-t_0}$:

$$\underline{g}_{i,t-t_0} = z_{i,t-t_0} + \underline{\xi}_{i,t-t_0}. \tag{4}$$

The signal component represents the imperfection of the (deterministic) trend with respect to the actual land subsidence. For many applications the modeling of this signal term is necessary, since the trend describes the true subsidence only to a first-order approximation. This stochastic quantity is also referred to as *model noise*. Using Eqs. (3) and (4) we may rewrite the leveling observation equation (1) as

$$\underline{h}_{ij,t} = -z_{i,t-t_0} + z_{j,t-t_0} - H_{i,t_0} + H_{j,t_0} + \underline{e}_{ij,t}, \tag{5}$$

where the random error $\underline{e}_{ij,t}$ is the following sum accounting for model noise and measurement noise: $\underline{e}_{ij,t} = -\underline{\xi}_{i,t-t_0} + \underline{\xi}_{j,t-t_0} + \underline{\varepsilon}_{ij,t}$. In an analogue manner, the vertical deformation observation equation (2) for InSAR can be rewritten as:

$$\underline{dH}_{k,t_l t_m} = -z_{k,t_l-t_0} + z_{k,t_m-t_0} - dH_{t_l t_m} + \underline{e}_{k,t_l t_m}, \tag{6}$$

where the random error $\underline{e}_{k,t_l t_m}$ is the following sum, accounting for model noise and measurement noise: $\underline{e}_{k,t_l t_m} = -\underline{\xi}_{i,t_l - t_0} + \underline{\xi}_{i,t_m - t_0} + \underline{\varepsilon}_{k,t_l t_m}$. Note that in contrast to Eq. (5) in Eq. (6) no initial heights are parameterized, since these are eliminated in case of InSAR-derived height differences.

3. A spatio-temporal trend model for land subsidence

For subsidence modeling above deep gas or oil reservoirs, smooth 7-parameter spatio-temporal subsidence bowls were successfully applied (Houtenbos, 2000). The subsidence at a point *i* at time *t* is then modeled as the following superposition of n_B subsidence bowls, where each bowl has an ellipsoidal shape in the horizontal plane and a Gaussian profile:

$$z_{i,t-t_0} = \sum_{B=1}^{n_B} z_{i,t-t_{0,B}} \quad \text{where } z_{i,t-t_{0,B}} = \begin{cases} 0, & t \le t_{0,B} \\ v_B (t - t_{0,B}) \exp\{-\tfrac{1}{2} r_{i,B}^2\}, & t_{0,B} \le t \le t_{e,B} \\ v_B (t_{e,B} - t_{0,B}) \exp\{-\tfrac{1}{2} r_{i,B}^2\}, & t \ge t_{e,B} \end{cases} \tag{7}$$

with $t_{0,B}, t_{e,B}$ the start and end time of the subsidence (of bowl *B*), v_B the velocity of subsidence in the center of the bowl, and $r_{i,B}$ the standardized radius from the center of bowl *B* to point *i*. Model (7) assumes that the bowl subsides with an unknown but constant velocity v_B, which exponentially decreases with increasing distance from the center of the bowl. The standardized radius reads:

$$r_{i,B}^2 = \left(\frac{(x_i - x_{c,B}) \sin\phi_B + (y_i - y_{c,B}) \cos\phi_B}{a_B} \right)^2 + \left(\frac{(x_i - x_{c,B}) \cos\phi_B + (y_i - y_{c,B}) \sin\phi_B}{b_B} \right)^2, \tag{8}$$

where (x_i, y_i) denote the known horizontal position of point *i*, $(x_{c,B}, y_{c,B})$ the position of the center of bowl *B*, whereas a_B, b_B and ϕ_B are the long respectively short axes and the orientation of ellipsoidal bowl *B*. Thus the parameters of interest per bowl, estimated in the processing, are the five parameters governing the *shape* and *position* of the bowl, i.e. a_B, b_B, ϕ_B and $(x_{c,B}, y_{c,B})$, plus the two *temporal* parameters, subsidence start time $t_{0,B}$ and subsidence velocity v_B. Sometimes also an eighth parameter is estimated, i.e. the subsidence end time $t_{e,B}$, but this parameter is only estimated when data are available beyond this time.

4. Trend-signal estimation and testing procedure

Equation (7) relates the leveling and InSAR observation equations (5) and (6) to the unknown parameters of interest. Because the observation equations are nonlinear in these subsidence parameters, they need to be linearized. After linearization, the model of observation equations reads:

$$\begin{bmatrix} \Delta \underline{h} \\ \Delta \underline{dH} \end{bmatrix} = \begin{bmatrix} WA_{sub} & WA_{hgt} & 0 \\ SA_{sub} & 0 & A_{sht} \end{bmatrix} \begin{bmatrix} \Delta p \\ \Delta H_{t_0} \\ \Delta dH_{dt} \end{bmatrix} + \begin{bmatrix} \underline{e}_h \\ \underline{e}_{dH} \end{bmatrix}. \tag{9}$$

In this model the observation vector consists of the vector of (linearized) leveling observations, $\Delta \underline{h}$, and the vector of (linearized) InSAR observations, $\Delta \underline{dH}$. The vector of unknown parameters consists of the vector of 7 (linearized) parameters per subsidence bowl, Δp, the vector of (linearized) leveling benchmark heights, ΔH_{t_0}, and the vector of (linearized) InSAR shift parameters, ΔdH_{dt}. In the design matrix, A_{sub} denotes the matrix with coefficients of the parameterized subsidence bowl(s). Because this matrix is set up at height level, it needs to be coefficient matrix for the benchmark heights and matrix A_{sht} the coefficient matrix for the InSAR shift parameters. Note that to estimate the initial benchmark heights, at least one of these

heights needs to be fixed (S-basis). The choice of this height does however not influence the estimated subsidence parameters. Finally, the vector of residuals contains the random noise terms of the leveling and InSAR observations. It is assumed that these noise components have zero mean. Model (10) is referred to as the *functional* model. Besides this functional model, for the processing a *stochastic* model is needed, in which the stochastic properties of the observations are taken into account. This stochastic model is determined by a combination of *measurement noise* and *model noise* (see Sect. 2).
The measurement noise of leveling observations is well known, and it is usually assumed that the variances of the observations are a linear function of the distance between the benchmarks. In addition, correlation between observations of the same epoch as well as between different epochs is assumed to be absent. The measurement noise of the InSAR-derived observations is assumed to be uncorrelated in time (so no correlation between independent deformation maps). Spatial correlation is modeled for observations per interferogram. This correlation is usually caused by differences in atmospheric conditions during the two InSAR acquisitions from which the deformation map is created (Hanssen, 2001). In the *SuMo* software for this spatial correlation an exponential function is used. The variances of the InSAR observations are derived from the estimated coherence, the multilook factor, and the estimated atmospheric variance.
To make the model fit the data, it is often necessary to add a part accounting for model noise to the stochastic model. Although the exact stochastic properties of model noise are unknown, both spatial and temporal correlations seem to be plausible assumptions. In the *SuMo* software model noise is modeled as a random-walk process in time and an exponential covariance function in space (Houtenbos, 2000).

With the functional and stochastic models specified, the best fitting subsidence model is determined in a stepwise procedure of *least-squares adjustment*, *statistical hypothesis testing* and *adaptation* of both the data and the model. In each step the actual model and data –the so-called *null-hypothesis* model– are tested against a number of alternative hypotheses, each suggesting a specific model adaptation or possible error(s) in the data. For an overview of these alternative hypotheses we refer to (Kenselaar, 2001).
When the null hypothesis is eventually accepted, the estimated subsidence *trend* at all points, denoted as $\hat{z}$, follows from inserting the estimated subsidence parameters into Eq. (7). Besides these trend estimates, it is also possible to estimate the model noise terms (the *signal*) at all points from the least-squares residuals of the trend model. With these estimates, denoted as $\hat{\xi}$, the *total subsidence* $\hat{g}$ at all points is finally computed as:

$$\hat{g} = \hat{z} + \hat{\xi} \tag{10}$$

For visualization purposes the subsidence is computed at a regular grid of points, instead of the irregular locations of the leveling benchmarks and/or InSAR pixels. Using such a grid it is easy to plot contour maps of the subsidence. In the *SuMo* software this is realized using *collocation* (Moritz, 1976). Using collocation it is also possible to compute the subsidence at other times than the times of the measurements (interpolation in between epochs, prediction to future epochs), see (Kenselaar and Quadvlieg, 2001).

3. Example: an isolated oilfield

To demonstrate the performance of an integrated approach, both leveling and InSAR data measured at an isolated oilfield in the Middle East were used. For this oilfield it is known that the subsidence can be modeled to a sufficient degree of approximation by *two* overlapping bowls. The subsidence is caused by the compaction of the oilfield. The subsurface shape of this phenomenon correlates very well with the subsidence bowls at the surface. From late 1998 until early 2002 a leveling network was yearly surveyed and a number of InSAR-derived deformation maps have been computed.

5.1 Leveling-only case

First the processing was carried out with leveling data only. All 4 epochs of data were used and after some minor adaptations the model under the null hypothesis was accepted. The 13 subsidence parameters, estimated from 199 leveling observations, are summarized in Table 1, together with their standard deviations. It is known that subsidence started before the epoch of the first leveling network, but since there are no data available before 29 December 1998 in the processing the start time of subsidence of bowl 1 was fixed at this date.
Table 1 shows that the subsidence velocity is estimated at about 4 cm/yr (with a standard deviation of about 0.5 cm/yr). The precision of bowl 2 is somewhat worse than that of bowl 1, mainly because there are less data from which bowl 2 are estimated. This is a consequence of the start time of the second bowl, the second half of August 2000.

Table 1. Estimated subsidence parameters from leveling-only processing

Leveling-only processing	Bowl 1		Bowl 2	
	Estimated value	Standard deviation	Estimated value	Standard deviation
$\hat{v}$ [mm/yr]	-34	3	-37	5
$\hat{t}_0$ [days]	29-Dec-1998	0	15-Aug-2000	43
$\hat{a}$ [m]	2805	203	2093	256
$\hat{b}$ [m]	1335	59	1409	145
$\hat{\phi}$ [gon]	40	3	131	11
$\hat{x}_c$ [m]	9189	144	6535	279
$\hat{y}_c$ [m]	8008	189	8135	181

Figure 1 visualizes the estimated trend, signal and sum of trend plus signal, the total subsidence, on the last epoch, 15 January 2002. For the visualization of the signal, collocation has been used. As can be seen, the superposition of the two bowls results in a 'heart-shaped' subsidence area. From the figures it seems that the estimated trend is in good agreement with the 'real' subsidence, since the magnitude of the signal is smaller than 1 cm at all places. Figure 2 shows the small discrepancies between trend and total subsidence for two profiles along the two black crossing lines in Fig. 1.

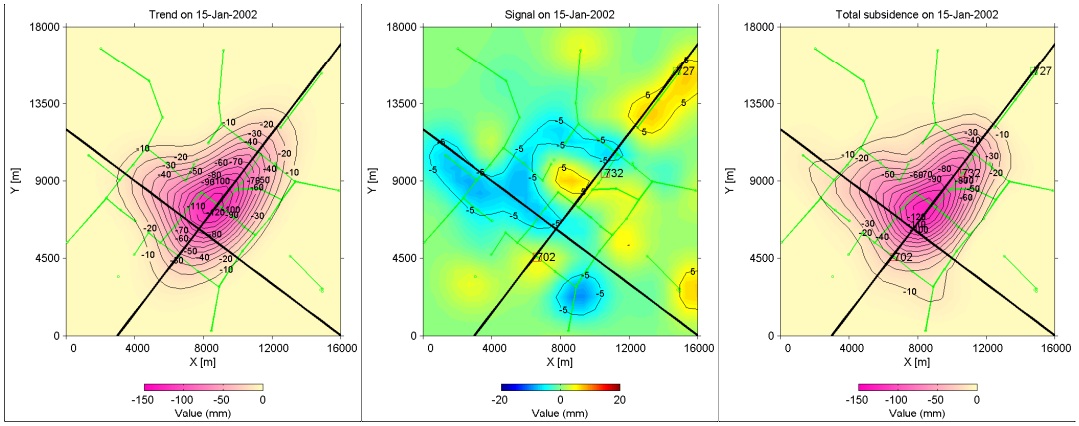

Fig. 1. Estimated subsidence (left: trend, middle: signal, right: total) since 1999, from a leveling-only processing on epoch 15 January 2002. The black contour lines give the subsidence in mm ranging from 10 to 120 mm. The green lines represent leveling lines, while for the two straight black lines vertical profiles are given in Fig. 2.

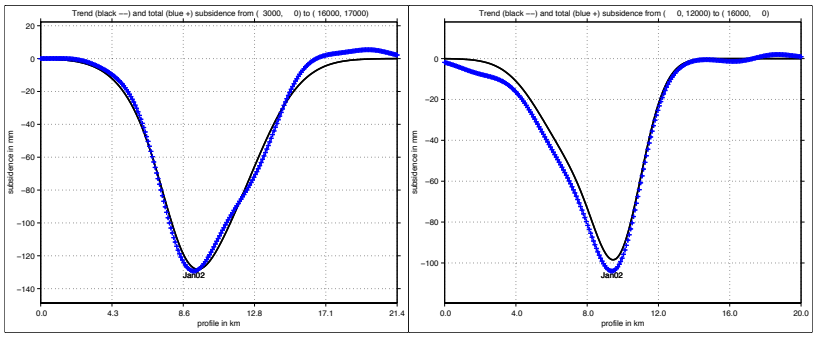

Fig. 2. Subsidence profiles for 15 January 2002: SW-NE profile (left) and NW-SE profile (right), corresponding to the black lines in the lower figures of Fig. 1.

5.2 Integrated leveling-InSAR case

Since the start of the subsidence InSAR data have been acquired over this area. Deformation maps are available for intervals up to about 1 year, with a (multi-looked) resolution of about 20 m. Due to the arid nature of the area, the scattering characteristics are quite stable resulting in rather coherent interferograms. See Hanssen (2001) for a background in the InSAR technique. To avoid computer memory problems it was necessary to restrict the number of InSAR data points (pixels) in the *SuMo* processing. Hence a data reduction step was carried out, in which only the pixels covering the subsidence area were selected. Instead of grids with 2500 x 2500 pixels (resolution: 20 m), we used much smaller grids, containing 30 x 26 pixels, with a resolution of 400 m. Using this resolution we believe that the information content in the original data is still sufficiently preserved.

Table 2. Information on InSAR data used in analysis

Deformation map	Time interval	Sensor	Wavelength
1	29/06/1999-21/12/1999 (175 days)	ERS-2	5.6 cm
2	01/10/2000-02/09/2001 (336 days)	Radarsat	5.6 cm

Since we do not have a deformation map available covering the complete time span from the beginning of 1999 until 2002, we used two InSAR deformation maps referring to shorter time intervals. Table 2 gives some information on the two maps. The estimated bowl parameters of the integrated *SuMo* processing of 199 leveling and 1514 InSAR observations are given in Table 3. This table also gives statistics of a test whether the estimated parameters significantly differ from their leveling-only counterparts in Table 1. This significance test decides that the difference between a parameter in this table, $\hat{x}_2$, and its leveling-only counterpart in Table 1, $\hat{x}_1$ is significant (with a significance level of 0.05) if $|\hat{x}_2 - \hat{x}_1| / \sqrt{\sigma^2_{\hat{x}_1} + \sigma^2_{\hat{x}_2}} > 2$ (hereby it is assumed that $\hat{x}_1$ and $\hat{x}_2$ are uncorrelated). Since the largest test statistic is 1.3 (orientation of bowl 2), the differences between the parameters of the integrated approach and the leveling-only processing were not found to be significant. Comparing the standard deviations of Table 3 with their counterparts in Table 1, it follows that the precision of bowl 1 is about the same in both cases, while the precision of bowl 2 is clearly better in the integrated approach. Obviously the InSAR data hardly contribute to the estimation of bowl 1. This can be explained by considering the times of beginning of the bowls in relation to the lengths of the deformation maps. While bowl 1 starts immediately from the beginning of 1999 and is well estimated from four leveling epochs, bowl 2, starting in August 2000, is covered by only two leveling epochs. Addition of a deformation map (1 October 2000 – 2 September 2001), which almost completely covers the time of development of bowl 2, significantly enhances the estimation of this bowl.

Table 3. Estimated subsidence parameters from integrated leveling-InSAR processing

Integrated leveling-InSAR	Bowl 1			Bowl 2		
	Estimated value	Stdev.	Sign.test[1]	Estimated value	Stdev.	Sign.test[1]
$\hat{v}$ [mm/yr]	-31	2	0.8	-40	4	0.5
$\hat{t}_0$ [days]	29-Dec-1998	0	0	07-Sep-2000	35	0.4
$\hat{a}$ [m]	2775	200	0.1	2237	213	0.4
$\hat{b}$ [m]	1369	64	0.4	1207	76	1.2
$\hat{\phi}$ [gon]	44	3	0.9	115	5	1.3
$\hat{x}_c$ [m]	9248	150	0.3	6714	234	0.5
$\hat{y}_c$ [m]	8094	172	0.3	8005	104	0.6

[1] With respect to leveling-only in Table 1.

In a search for more efficient monitoring strategies it is probably more interesting to analyze an integrated approach not using *all* leveling epochs. Therefore another integrated processing was carried out, using the same two InSAR deformation maps, but with only *two* leveling epochs: 29 December 1998 and 15 January 2002 (In the leveling-only case at least *three* epochs are needed for the estimation of two subsidence bowls). This integrated approach resulted in a precision of the bowl parameters of at most only 1.2 times worse than their counterparts in Table 2. An exception to this are the start time and velocity of bowl 2, which were about a factor 4 worse than their counterparts in Table 2. This large deterioration is a consequence of the fact that it is not possible to estimate the start time of subsidence from the InSAR height differences (see also the observation equation for InSAR in Sect. 2). So in the integrated approach this time is purely determined by the leveling data. Since the estimated velocity of bowl 2 is highly correlated with the estimated start time, the precision of this parameter is worsened with a similar factor.

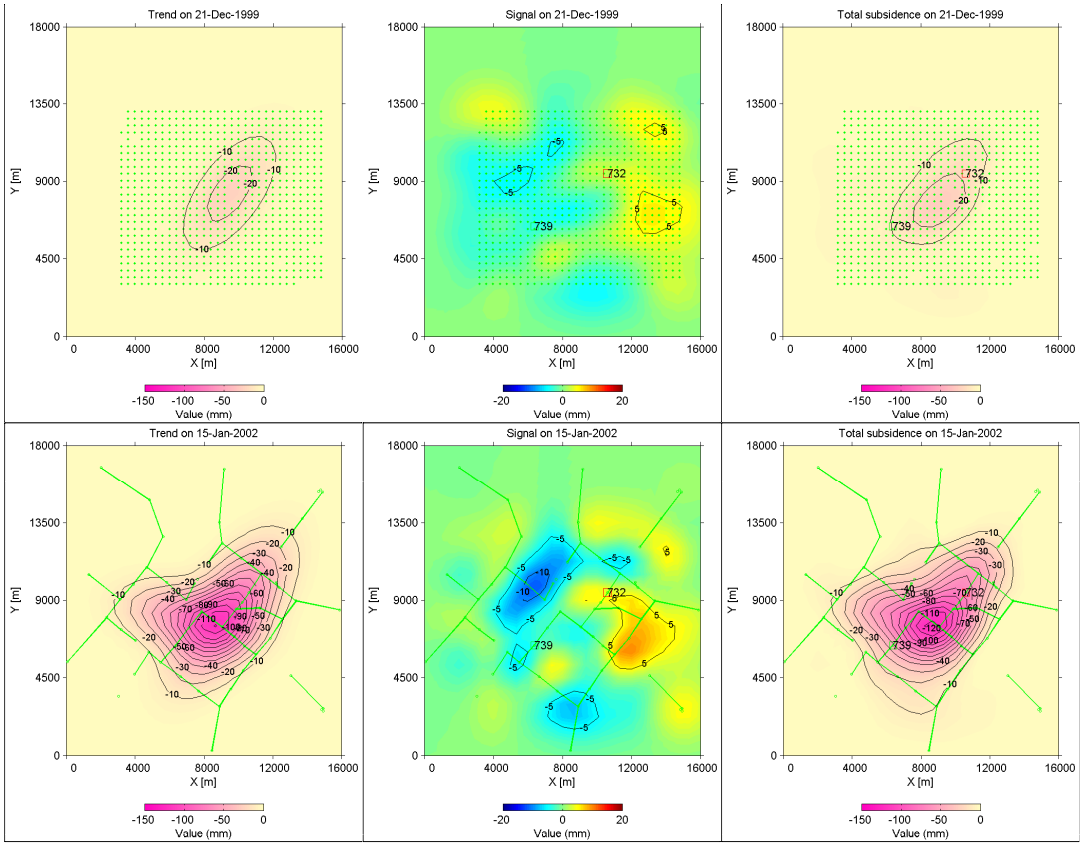

Fig. 3. Estimated trend (left), signal (middle) and total (right) subsidence using integrated leveling-InSAR data, for 21 December 1999 (upper three figures) and 15 January 2002 (lower three figures).

Figure 3 depicts the collocated subsidence on two epochs using the integrated approach of two leveling epochs and two InSAR deformation maps. Although the magnitude of the signal is larger than in case of leveling only (Fig. 1), it is still at most only 1 cm.

5.3 InSAR-only case

In the previous section it was explained that leveling data are needed to determine the start time of subsidence. If this time is known for both bowls, then the other parameters may also be estimated from InSAR data *only*, thus without any leveling data included. Another *SuMo* processing was performed based on the two deformation maps, fixing the start time of bowl 2 on 1 September 2000 (bowl 1 still fixed on 29 December 1998). The results were that all estimated parameters were in agreement with those of Table 2, according to the significance test, and that the precision of bowl 1 was 1.5 times worse, while the precision of bowl 2 was only 1.1 times worse than their counterparts in Table 2.

4. Concluding remarks

In this paper it has been shown that a trend-signal procedure, which has been successfully applied for the estimation of subsidence due to gas or oil extraction from precise leveling data, is also suitable for an integrated approach of both leveling and InSAR data. It is in principle possible to apply the method to InSAR data only, provided that these data cover the time span of subsidence sufficiently and that the InSAR data are of good quality. However, since the SAR satellites and sensors have not yet reached an operational and reliable level, it is better not to rely on InSAR data only for the time being, so combining leveling and InSAR seems to be the best option. In this paper it was shown that the amount of leveling data could be drastically reduced in the integrated approach, compared to a leveling-only estimation. More research should focus on how the amount of leveling data may be reduced even further, possibly by using less redundant network designs.

Acknowledgements

This work is performed within project 2.4 ‘Integrated Deformation Analysis’ of the DIOC (*Delft Interfaculty Research Center*) research program ‘Determination and Prediction of the 3D movements of the Earth’s Surface’ from Delft University of Technology. The *Nederlandse Aardolie Maatschappij* (NAM) is gratefully acknowledged for the cooperation during the development of the *SuMo* software and providing the data used in this study.

References

Hanssen, R.F. (2001). *Radar Interferometry: Data interpretation and error analysis*. Kluwer Academic Publishers, Dordrecht, 308 p.

Houtenbos, A.P.E.M. (2000). The quantification of subsidence due to gas extraction in the Netherlands. *Land Subsidence, Proceedings of the IAHS Sixth International Symposium on Land Subsidence (SISOLS),* Italy, 177-189.

Kenselaar, F. (2001). A testing procedure for subsidence analysis. *Proceedings of the 10th FIG International Symposium on Deformation Measurements,* USA, 40-49.

Kenselaar, F. and R. Quadvlieg (2001). Trend-signal modelling of land subsidence. *Proceedings of the 10th FIG International Symposium on Deformation Measurements,* USA, 336-345.

Moritz, H. (1976). Least squares collocation. *Manuscripta Geodaetica*, Vol. 1, 1-40.

Odijk, D. and F. Kenselaar (2002). *Subsidence Modelling, user’s manual of the SuMo software (version 4)*. Delft University of Technology, 66 p.